

S1

Electronic Supporting Information (ESI) for:

The interplay of Iron (II) Spin Transition and Polymorphism

Ivan Šalitroš^{a,b}, Olaf Fuhr^a, Andreas Eichhöfer^a, Robert Kruk^a, Ján Pavlik^b, Lubor Dlháň^b, Roman Boča^b and Mario Ruben^{a*}

a)Institut für Nanotechnologie, Karlsruher Institut für Technologie, Postfach 3640, 76021 Karlsruhe, Germany

*E-mail: mario.ruben@kit.edu

b)Faculty of Chemical and Food Technology, Institute of Inorganic Chemistry, Technology and Materials, Slovak University of Technology, Bratislava 812 37, Slovak Republic

c) Institute de Physique et Chimie de Matériaux de Strasbourg (IPCMS), CNRS-Université de Strasbourg, 23, rue du Loess, BP 43 67034 Strasbourg cedex 2 France

Table of Contents

S.No.	Contents	Page No.
1	FT IR and UV/VIS absorption spectroscopy of $[\text{Fe}(\text{L})_2](\text{BF}_4)_2$	S2
2	Hydrogen bonds and short contacts distances in polymorphic compounds $[\text{Fe}(\text{L})_2](\text{BF}_4)_2$	S2
3	Variable temperature X-ray powder diffractograms of polymorphic $[\text{Fe}(\text{L})_2](\text{BF}_4)_2$	S4

S2

1. Infrared spectroscopy of $[\text{Fe}^{\text{II}}(\text{L})_2](\text{BF}_4)_2$

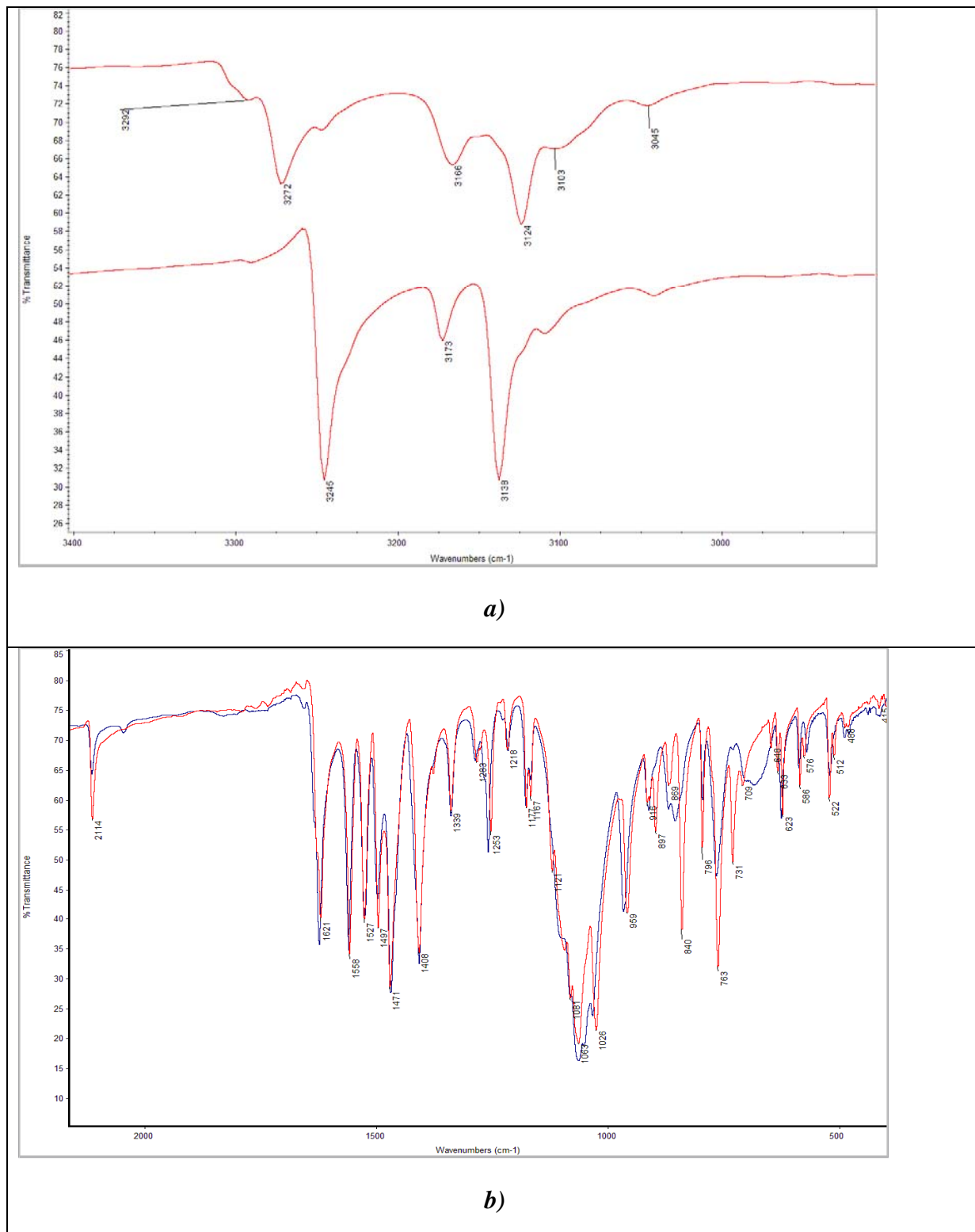


Figure S1 FTIR spectra of polymorphic compound $[\text{Fe}^{\text{II}}(\text{L})_2](\text{BF}_4)_2$: *a*) comparison of spectra differences between **1A** (bottom) and **1B** (top) *b*) the finger print area of IR spectrum for **1A** (blue line) and **1B** (red line)

S3

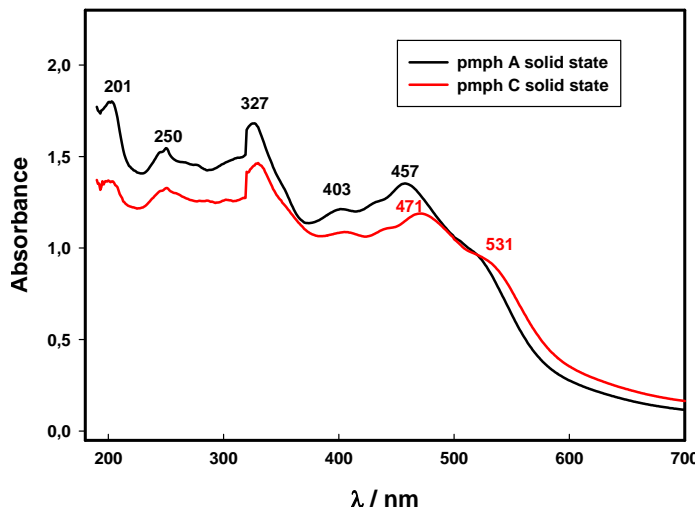


Figure S2 Solid state room temperature UV/VIS spectra of polymorphs **1A** and **1B**

2. Hydrogen bonds and short contacts distances in polymorphic compound $[\text{Fe}^{\text{II}}(\text{L})_2](\text{BF}_4)_2$

Polymorph **1A**

	F–C	F–H	angle (F–C–H)
F1B5	3.3194(5)	2.5016(4)	144.345(405)
F1B27	3.2219(6)	2.3046(4)	162.139(399)
F2C27	3.4598(5)	2.8510(5)	122.793(330)
F4C1	3.0933(4)	2.3914(3)	130.485(408)
F4C29	3.0625(5)	2.3130(3)	135.253(380)
F2C10	3.1424(6)	2.3935(4)	135.490(428)
F3C3	3.2224(5)	2.2930(4)	165.848(366)
F3C31	3.0983(6)	$\pi\pi$ stacking	125.369(571) (F3-C30C31B32)
F2C52	3.2617(5)	2.3535(4)	159.808(408)
F3C3	3.2224(5)	2.2930(4)	165.848(366)
F8C20	3.2841(4)	2.3618(3)	163.675(372)
F5C22	3.3234(5)	2.4537(4)	155.289(397)
F6C42	3.0111(5)	2.4352(3)	118.873(24)
F7C15	3.0462(6)	2.4983(4)	116.734(18)
F7C40	3.3990(5)	2.5731(4)	116.662(430)
F6C23	3.3179(6)	2.8099(6)	114.662(430)
F9C14	3.1738(6)	2.2405(4)	167.198(400)
F9C33	3.3230(4)	2.2405(4)	158.788(374)
F12C50	3.2053(4)	2.5390(3)	127.439(398)

F12C9	3.0523(5)	2.3798(3)	127.439(383)
F10C35	3.2568(5)	2.3412(3)	161.720(357)
F11B41	3.0210(5)	2.5727(4)	109.204(431)

S4

F13C48	3.0115(5)	2.3050 (3)	158.742(399)
F14C16	3.0998(4)	2.5058(3)	130.600(386)
F14C37	3.2329(6)	2.2965(3)	120.701(396)
F15C11	3.1231(5)	2.3058(4)	168.517(484)
F16C28	3.2471(5)	2.3432(3)	143.741(395)

Polymorph 1B

	F–C	F–H	angle (F–C–H)
F1B4	3.2652(4)	$\pi\pi$ stacking	130.954(12) (N2C4C5-F1)
F1B8	3.3153(6)*	2.4755(4)	152.678(16)
F2C5	3.0900(4)	2.8140(4)	135.753(7)
F1'C4	3.2652(4)	$\pi\pi$ stacking	130.954(12) (N2C4C5-F1')
F1'C8	3.3153(6)*	2.4755(4)	152.678(16)
F2'C5	3.0900(4)	2.8140(4)	135.753(7)

Polymorph 1C

	F–C	F–H	angle (F–C–H)
F3AC2	3.2141(193)	2.4114(122)	144.492(541)
F3AC13	2.4114(122)	2.4241(130)	152.792(512)
F3CC9	3.0223(186)	2.1007(176)	171.792(675)
F1CC9	3.5213(144)	2.4359(119)	159.204(570)
F1AC9	3.3455(144)	2.4935(118)	152.480(571)
F1BC7	3.2376(253)	2.3800(247)	153.265(688)
F2BC1	3.0769(247)	2.3085(235)	139.670(767)
F1BC1	3.2559(264)	2.3374(250)	169.353(797)
F3BC1	3.0549(170)	2.2678(156)	142.007(611)
F3BC2	3.1262(158)	2.2342(137)	160.503(578)
F2CC5	3.1144(205)	2.4503(169)	128.378(582)
F4BC5	3.2481(192)	2.4868(182)	141.486(559)
F4AC3	3.0619(160)	2.3364(146)	134.534(586)
F4BC3	3.0311(110)	2.2946(175)	135.689(659)
F4AC11	3.1911(147)	2.4801(136)	133.344(509)
F4BC11	3.0650(193)	2.3614(184)	132.217(601)
F1CC5	3.0239(136)	$\pi\pi$ stacking	124.726 (614) [°] (F1-BC4C5C6)

S5

3. Variable temperature X-ray powder diffractograms of polymorphic $[\text{Fe}^{\text{II}}(\text{L})_2](\text{BF}_4)_2$

The polymorphic compound $[\text{Fe}^{\text{II}}(\text{L})_2](\text{BF}_4)_2$ was studied by temperature-dependent powder diffraction studies at various temperatures. At the beginning, the investigated material was tetragonal **1B** polymorph, which was examined in two following heating/cooling temperature cycles. At the first, the sample was heated from 300 K to 460 K and then cooled down to room temperature. At 490 K, the reflections of tetragonal **1B** polymorph vanished and the resulting powder pattern is in agreement with those two calculated for the two orthorhombic phases (**1A** and **1C**) whereas the broadness of the peaks does not allow for a further differentiation (Fig. S4). In the second temperature cycle, the orthorhombic phase, arisen from the first temperature variable diffraction experiment, was overheated up to 493 K in order to investigate reversibility of the previous **1B**→**1C** transition. But heating up to 493 K and consequential cooling down to room temperature caused only slight shifts of reflections which are attributed to the change of lattice constants and result in the conclusion of the irreversibility of the **1B**→**1C** phase transition.

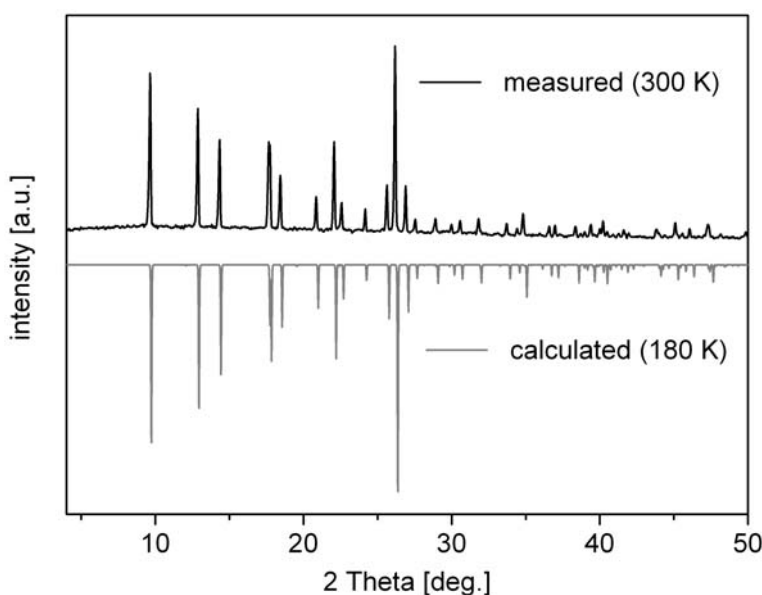


Figure S3 Room temperature X-ray powder pattern of the polymorph **1B** (up) compared to the corresponding calculated pattern from single crystal X-ray data taken at 180 K (down).

S6

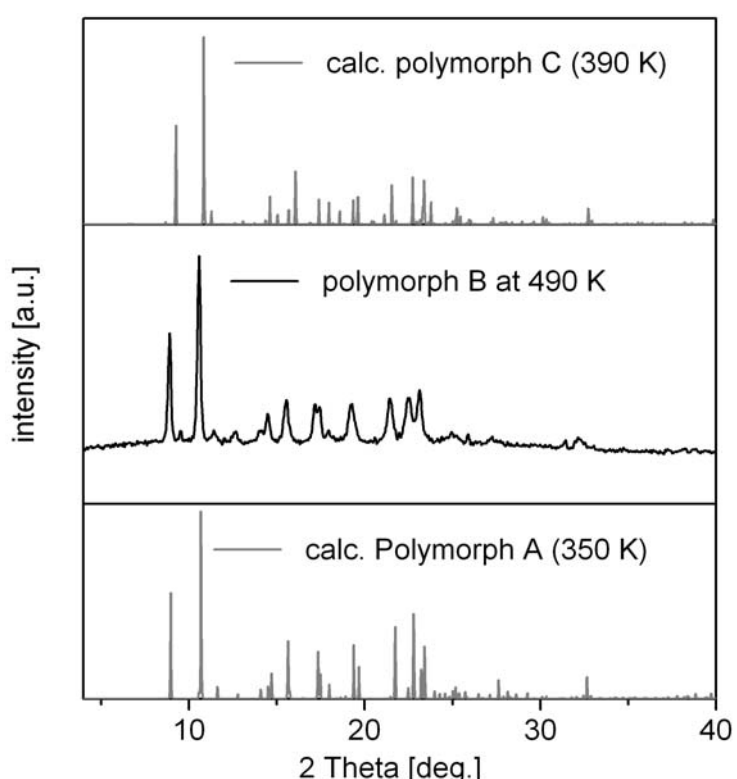


Figure S4 High temperature powder pattern of the polymorph **1B** heated to 490 K (center) compared to the calculated patterns of polymorph **1A** (down) and **1C** (up) from single crystal X-ray data taken at 350 and 390 K respectively.